^{14}N MAS NMR Spectroscopy and Quadrupole Coupling Data in Characterization of the IV ↔ III Phase Transition in Ammonium Nitrate

Tania Giavani, Henrik Bildsøe, Jørgen Skibsted, and Hans J. Jakobsen*

Instrument Centre for Solid State NMR Spectroscopy, Department of Chemistry, University of Aarhus, DK-8000 Aarhus C, Denmark

Received: August 30, 2001; In Final Form: December 20, 2001

The first application of ^{14}N MAS NMR spectroscopy and the associated ^{14}N quadrupole coupling data for characterizing a phase transition between two solid phases is presented. For NH_4NO_3, the transition between the phases IV and III at about 35 °C and the phases themselves are studied by ^{14}N MAS NMR using the NH_4^+ as well as the NO_3^- ion as probes. Spectra are acquired employing spinning speeds in the range from 2000 to 7000 Hz thereby taking advantage of the frictional heating as the heat source. The ^{14}N quadrupole coupling constants and asymmetry parameters for both the NH_4^+ and NO_3^- ion determined from these spectra show large changes upon transition between the two phases. Also the transition exhibits the effect of hysteresis with a deviation of about 10 °C for the transition temperature. The results show great potential for ^{14}N MAS NMR being a useful tool in characterizing phase transitions for nitrogen compounds from ^{14}N quadrupole coupling data.

Introduction

In a recent communication,[1] it has been demonstrated that solid-state magic-angle spinning (MAS) NMR spectroscopy of the important ^{14}N spin isotope (99.63% natural abundance, spin $I = 1$) can be lifted to a level of high usefulness in chemistry and materials science. Generally, the low-γ ^{14}N quadrupolar nucleus is considered a most difficult nucleus to be studied by solid-state NMR methods, in particular by the high-resolution techniques of MAS NMR. One reason that makes ^{14}N NMR a much greater challenge, as compared to other low-γ quadrupolar nuclei, is the fact that it does not possess a central transition (integer spin isotope), i.e., the commonly investigated transition for low-γ quadrupolar nuclei (e.g., ^{17}O, ^{35}Cl, ^{39}K, ^{25}Mg, ^{43}Ca, ^{67}Zn, ^{95}Mo, and ^{137}Ba). However, taking advantage of state-of-the-art transmission line tuning (TLT) CP/MAS probes at high magnetic fields, we recently showed that ^{14}N quadrupolar coupling constants (C_Q) in the range 0.5−1.0 MHz (or even larger) and their associated asymmetry parameters (η_Q) may be determined from the intensities and line shapes of the numerous spinning sidebands (ssbs) observed for the ($1 \leftrightarrow 0$) and ($0 \leftrightarrow -1$) transitions in MAS experiments. In addition to the required high stability in sample spinning, we should note that the TLT probe tuning technology greatly contributes to the quality of the spectra by reducing acoustic ringing usually hampering the observation of low-γ nuclei employing high-Q MAS probes with ceramic capacitors as tuning elements.

Ammonium nitrate (NH_4NO_3), a chemical of high industrial importance because of its use in agriculture and explosives, has been extensively investigated by several physical methods.[2] The great interest devoted to studies of this material originates from the unusually large number of phases (five) observed for solid NH_4NO_3 in the temperature range from −25 to 150 °C.[3−5] In particular, the phase transition just above room temperature (at about 35 °C) is of interest because it invokes breakage and caking of NH_4NO_3 pellets, thereby causing problems in the storage of this material. These studies include solid-state ^{15}N NMR spectroscopy employing ^{15}N-labeled NH_4NO_3 materials.[6,7] Recently a comprehensive variable-temperature (VT) solid-state ^{15}N NMR study (using MAS and static powder samples) characterizing the five accessible phases by their isotropic and anisotropic ^{15}N chemical shift parameters has been performed.[8]

In this work, we demonstrate the potential of solid-state ^{14}N MAS NMR spectroscopy as a tool in studies of phase transitions for nitrogen containing compounds. In addition to characterizing phase transitions by changes in isotropic chemical shifts as has been done by ^{15}N MAS NMR,[7−9] ^{14}N MAS NMR experiments allow determination of the ^{14}N quadrupole coupling parameters C_Q and η_Q. Such data constitute a valuable set of parameters characterizing the environment of the nitrogen atom and thus serve useful in distinguishing structural changes induced by a phase transition. Considering the phase transition in NH_4NO_3 from phase IV to phase III at about 35 °C, we show that ^{14}N MAS NMR spectroscopy of the ammonium (NH_4^+) as well as of the nitrate (NO_3^-) ion allow determination of quite different ^{14}N quadrupole coupling parameters (C_Q and η_Q) for these ions in the two phases. Because of a lack in VT hardware for performing a study at high/low temperatures for the other phase transitions in NH_4NO_3, the phase transition observed here at about 35 °C serves as an illustrative example of the first of its kind detected by ^{14}N MAS NMR spectroscopy. This phase transition was induced by the frictional heating of the sample/rotor[10] obtained for different rotor spinning speeds and exhibited a clear hysteresis effect.

Experimental Section

Materials. Because of a heavy overlap in the ^{14}N MAS NMR spectrum between the two manifolds of spinning sidebands arising from the NH_4^+ ion and the NO_3^- ion, two different samples of NH_4NO_3 were used in this study. A sample of ordinary, naturally occurring NH_4NO_3 (sample **1**), purchased from Merck, was used for the observation of the NH_4^+ ion.

* To whom correspondence should be addressed. Phone: +45 8942 3842. Fax: +45 8619 6199. E-mail: hja@chem.au.dk.

10.1021/jp013355t CCC: $22.00
Published on Web 02/21/2002

However, for the observation of the ^{14}N MAS spectrum for the NO_3^- ion without interference from the NH_4^+ ion, a sample of $^{15}NH_4^+$-enriched (99% ^{15}N) $^{15}NH_4NO_3$ (sample **2**), purchased from Isotec Inc., was used.

^{14}N MAS NMR Spectroscopy. ^{14}N MAS NMR experiments were performed at 43.34 MHz on a Varian INOVA-600 spectrometer with a 14.1 T widebore magnet using a Varian/Chemagnetics broadband low-γ frequency 7.5 mm T3 CP/MAS probe (loaded Q∼200 with low-pass filter) with transmission-line tuning and a specified maximum spinning speed of 7 kHz. Spinning speeds in the range from 2000 to 7000 Hz were employed. From the experimental results it was observed that the spinning speed of the 7.5 mm o.d. zirconia rotor could be stabilized to <0.1 Hz using the Varian/Chemagnetics MAS speed controller in the automated mode, i.e., to a higher precision than indicated by the ±1 Hz of the frequency counter. This was judged from the line widths of the extremely well-resolved line shapes observed within the individual ssbs far away from the isotropic resonance (e.g., ssb number forty). The pressure of the spinning gas (dried and oil-free ordinary air compressed to 8 bar) was highly stabilized by passing through three 50 l ballast tanks in series, each regulated to decrease the pressure by 0.5 bar before entering the MAS speed controller. It is believed that this highly stabilized air pressure is the main reason for the excellent spinning stability manifested by the MAS speed controller. The magic angle was adjusted to the highest possible accuracy (i.e., about <±0.015°) employing the ^{14}N MAS NMR spectrum of $(NH_4)_2HPO_4$, which should give the best possible resolution of the two different ^{14}N resonances for this sample. Spectra were recorded using single-pulse excitation with τ_p equal to 2.0 and 0.5 μs ($\gamma B_1/2\pi = 40$ kHz corresponding to $\tau_p^{90} = 6.3$ μs) for the NH_4^+ and NO_3^- ion, respectively. Spectral widths of 0.5 (NH_4^+) and 1.0 MHz (NO_3^-) were employed for the two ions with an acquisition of 50 ms and a repetition delay of 4 s for both FIDs which were zero-filled to 512k points before FT. ^1H decoupling ($\gamma B_2/2\pi = 50$ kHz) was used during acquisition of all ^{14}N MAS spectra employing a high-power low-pass filter (K&L Microwave, Inc.) on the ^{14}N observe channel of the probe, ^{14}N chemical shifts are referenced to the narrow ^{14}N MAS resonance (∼0.3 ppm) of an external sample of solid NH_4Cl. Sample temperatures for the different spinning speeds were determined with a precision of ±2 °C using a sample of ethylene glycol as described earlier.[10]

Simulations. All experimental ^{14}N MAS NMR spectra have been analyzed by computer simulations/iterative fittings on a Sun Microsystems Ultra 5 workstation using the program STARS, a solid-state NMR software package developed in our laboratory[11−15] and incorporated into the Varian VNMR software. Because of the low ^{14}N resonance frequency, even at 14.1 T ($\nu_0 = 43.34$ MHz), and the high Q (∼200) of the ^1H-X MAS probe system, the acquisition of ^{14}N MAS NMR spectra are far from ideal. For example, under our experimental conditions, the radio frequency (rf) bandwidth is highly suppressed during acquisition of the FID (i.e., 50% reduction for a width of $\nu_0/Q = 43.34/200 = 215$ kHz) compared to the corresponding bandwidth for detection at much higher frequencies (e.g., ^{23}Na or ^{27}Al) for the same Q value. This effect has already been incorporated into the original version of STARS. To achieve optimizations almost to perfection under these conditions, the original version of the STARS/VNMR program has been modified to include (i) variation in the rf offset for detection/excitation to compensate for nonideal cable length in the duplexer of the preamplifier, which will otherwise result in a "tilt" of the manifold of spinning sidebands (ssbs), (ii) a phase shift, dubbed "*Q* phasing", introduced by the narrow rf bandwidth and thus partly caused by the high Q of the probe system, and (iii) the second-order cross term between the quadrupole coupling and chemical shift anisotropy (CSA) in the average Hamiltonian (vide infra), a term proportional to $\nu_0\delta_\sigma C_Q/\nu_0$ and usually neglected,[13] but of importance for the appearance of the line shapes for the individual ssbs in ^{14}N MAS NMR of the nitrate ion.[1]

The quadrupole coupling and CSA parameters determined or used by STARS are related to their tensor elements by the following equations:

$$C_Q = \frac{eQV_{zz}}{h}$$

$$\eta_Q = \frac{V_{yy} - V_{xx}}{V_{zz}} \qquad (1)$$

$$\delta_\sigma = \delta_{iso} - \delta_{zz}$$

$$\eta_\sigma = \frac{\delta_{xx} - \delta_{yy}}{\delta_\sigma}$$

where $\delta_{iso} = {}^1/_3(\delta_{xx} + \delta_{yy} + \delta_{zz})$. The principal tensor elements of the CSA (δ) and electric field gradient (V) tensors are defined using the convention

$$|\lambda_{zz} - 1/3\mathrm{Tr}(\lambda)| \geq |\lambda_{xx} - 1/3\mathrm{Tr}(\lambda)| \geq |\lambda_{yy} - 1/3\mathrm{Tr}(\lambda)| \quad (2)$$

where $\lambda_{ii} = \delta_{ii}$ and V_{ii}. The Euler angles (ψ, χ, and ξ), describing the orientation of the CSA tensor relative to the quadrupole coupling tensor, correspond to positive rotations about $\delta_{zz}(\psi)$, the new $\delta_{yy}(\chi)$, and the final $\delta_{zz}(\xi)$ axis. These angles are defined in the ranges $0 \leq \psi \leq \pi$ and $0 \leq (\chi,\xi) \leq \pi/2$.[14]

Expressions for the first-order quadrupole and anisotropic shift Hamiltonians and for the second-order quadrupolar Hamiltonian are given in refs 12 and 13. The second-order quadrupolar-CSA cross term required for the simulations of the NO_3^- ion spectra arises from the general expression

$$\bar{\tilde{H}}^{(2)}(t) = \frac{-i\omega_0}{4\pi}\int_0^{2\pi/\omega_0}\int_0^t [\bar{\tilde{H}}(t),\bar{\tilde{H}}(t')]\,dt'\,dt = \frac{-i\omega_0}{4\pi}\int_0^{2\pi/\omega_0}\int_0^t ([\bar{\tilde{H}}_Q(t),\bar{\tilde{H}}_Q(t')] + [\bar{\tilde{H}}_Q(t),\bar{\tilde{H}}_\sigma(t')] + [\bar{\tilde{H}}_\sigma(t),\bar{\tilde{H}}_Q(t')] + [\bar{\tilde{H}}_\sigma(t),\bar{\tilde{H}}_\sigma(t')])\,dt'\,dt \quad (3)$$

where $\bar{\tilde{H}}^{(2)}(t)$ is the average Hamiltonian in the Zeeman interaction representation and $\omega_0 = 2\pi\nu_0$ is the Larmor frequency. The second and third terms of eq 3, which constitute the cross term, may be written as

$$\bar{\tilde{H}}^{(2)}_{Q,\sigma}(t) = -[A^Q_{2,1}(t)A^\sigma_{2,-1}(t) + A^Q_{2,-1}(t)A^\sigma_{2,1}(t)](I(I+1) - 3I_z^2)/\omega_0 \quad (4)$$

where $A^\lambda_{2,m}(t)$ denotes the spatial part of the interaction in the laboratory frame. The $A^\lambda_{2,m}(t)$ terms are obtained from the principal axis components and from the Euler angles defined above via Wigner rotations.[16]

Results and Discussion

A series of ^{14}N MAS NMR spectra with spinning speeds (ν_r) in the range from 2000 to 7000 Hz has been recorded for both

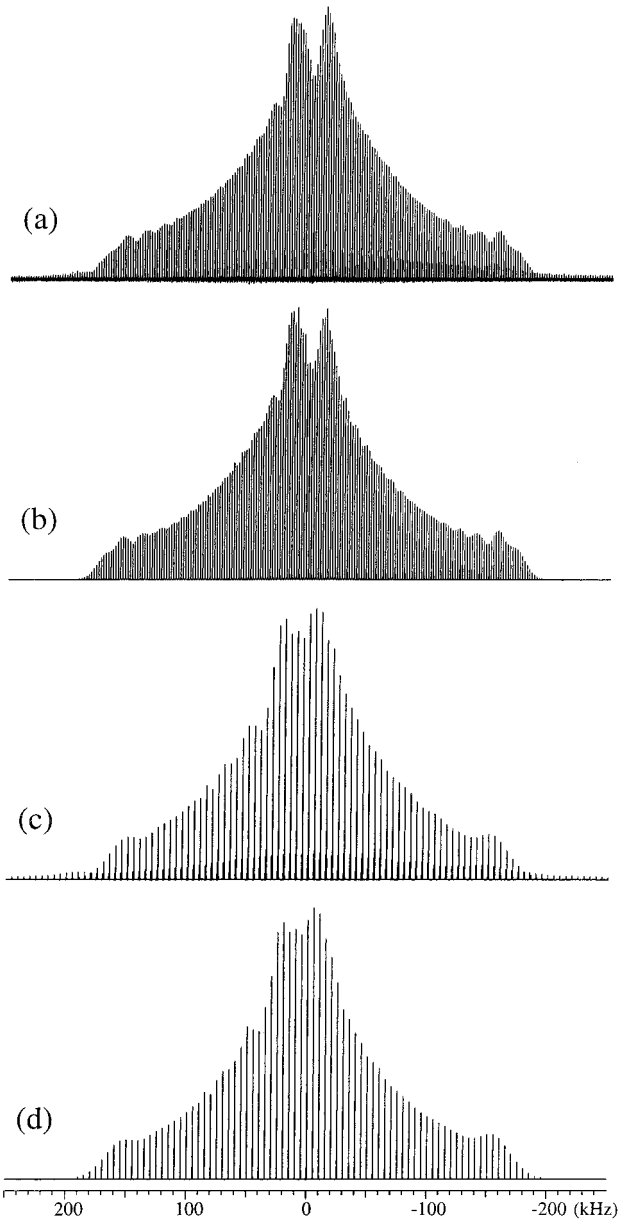

Figure 1. ^{14}N MAS NMR spectra of the NH_4^+ ion in ordinary NH_4NO_3 at two different spinning speeds. (a) Experimental spectrum for ν_r = 2000 Hz, a line broadening of 10 Hz, and 11 475 scans. (c) Experimental spectrum for ν_r = 5000 Hz, a line broadening of 10 Hz, and 2000 scans. Parts b and d illustrate the optimized simulated spectra corresponding to the experimental spectra in parts a and c, respectively, and to the parameters in Table 1. In addition to the experimental conditions given in the Experimental Section, the deviations from the exact magic angle were determined to be −0.015° for parts a and b and −0.010° for parts c and d. See also text.

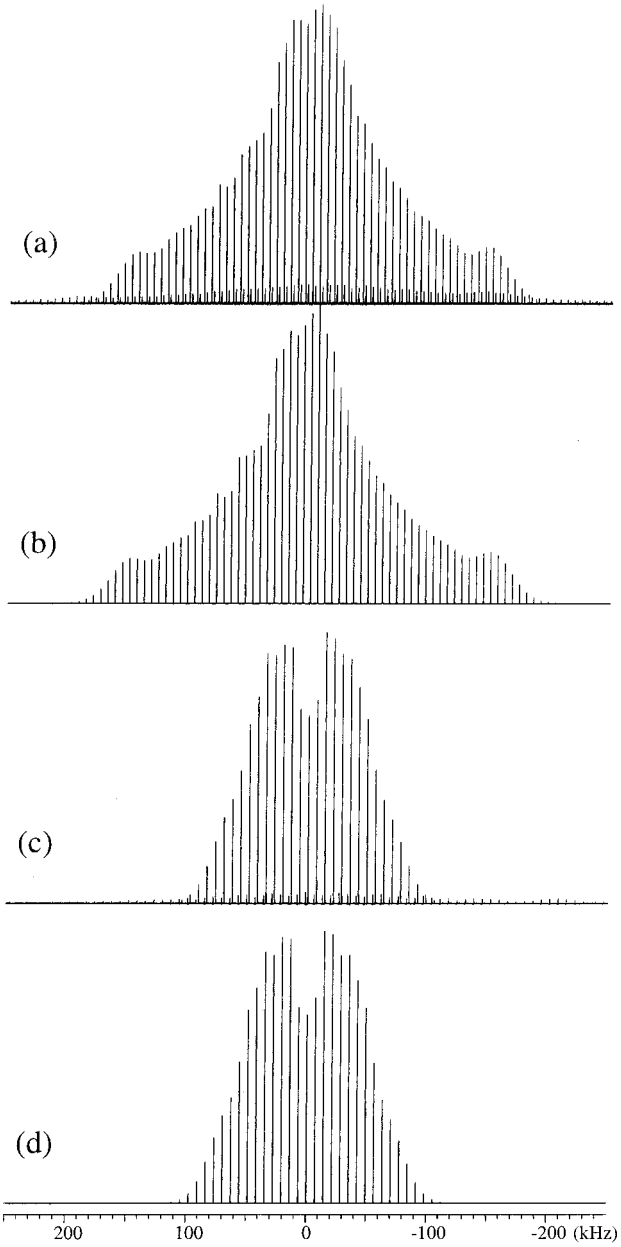

Figure 2. ^{14}N MAS NMR spectra of the NH_4^+ ion in ordinary NH_4NO_3 illustrating the phase transition from phase IV to III in going from ν_r = 6000 to 7000 Hz. (a) Experimental spectrum for ν_r = 6000 Hz, a line broadening of 10 Hz, and 928 scans. (c) Experimental spectrum for ν_r = 7000 Hz, a line broadening of 10 Hz, and 789 scans. Parts b and d show the optimized simulated spectra corresponding to parts a and c, respectively, the parameters in Table 1, and for deviations from the exact magic angle of −0.010° parts a and b and −0.009° parts c and d. A low-intensity manifold of ssbs from the NO_3^- ion is observed in the experimental spectra (see also text).

sample **1** and sample **2** with the purpose of characterizing the phase transition for NH_4NO_3 at about 35 °C by the spectra of the NH_4^+ ion as well as for the NO_3^- ion.

^{14}N MAS NMR of NH_4^+. Figures 1 and 2 show a series of experimental ^{14}N MAS NMR spectra for the NH_4^+ ion in sample **1** acquired in the order of increasing spinning speed using ν_r = 2000 Hz (Figure 1a), ν_r = 5000 Hz (Figure 1c), ν_r = 6000 Hz (Figure 2a), and ν_r = 7000 Hz (Figure 2c). Below each experimental spectrum is shown the simulation corresponding to the optimized parameters (Table 1) resulting from an iterative fit of the experimental spectrum. In all cases, the spectra exhibit an excellent agreement between experiment and simulation and thereby serve to illustrate the high quality of the corresponding parameters. We should note that a low-intensity manifold of ssbs, extending outside the spectral range for NH_4^+ and which arise from the NO_3^- ion, are observed in all experimental spectra. Also, it is pointed out that all simulations performed in relation to the analysis of the NH_4^+ ion spectra were carried out without including any CSA. Despite this, many of the slight asymmetries (with respect to the center of the experimental spectra) observed for the peak heights of the ssbs also turn up in the simulations. These variations are ascribed to slight differential line splittings/broadening for the ssbs across the spectral manifolds and are attributable to slight deviations (∼0.01°) in the spinning axis from the exact setting to the magic

TABLE 1: ^{14}N Quadrupole Coupling Parameters (C_Q, η_Q) and Isotropic Chemical Shifts (δ_{iso}) for the NH_4^+ and NO_3^- Ion in NH_4NO_3 at Different Spinning Speeds (ν_r) and Corresponding Sample Temperatures (t_c)[a]

ion	ν_r [kHz]	t_c[b] [°C]	figure	C_Q [kHz]	η_Q	δ_{iso}[c] [ppm]
NH_4^+ [d]	2.0	23	1a	246	0.85	−17.3
	5.0	31	1c	245	0.85	−17.6
	6.0	36	2a	245	0.85	−17.1
	7.0	41	2c	127	0.41	−15.8
NO_3^- [e]	7.0	41	3c	665	0.00	338.6
	6.0	36	4a	662	0.01	338.9
	5.0	31	4c	662	0.01	338.9
	4.0	28	3a	620	0.25	335.3

[a] The error limits for C_Q, η_Q, and δ_{iso} are ±10 kHz, ±0.01, and ±0.3 ppm, respectively. [b] The error in t_c is ±2 °C. [c] The δ_{iso} values (relative to solid NH_4Cl) include corrections for the second-order quadrupole shifts, which for the NH_4^+ ion are 3.0 ppm (phase IV) and 0.7 ppm (phase III) and for the NO_3^- ion are 15.7 ppm (phase IV) and 17.7 ppm (phase III). [d] Experiments for NH_4^+ are performed in order of increasing ν_r, i.e., increasing t_c, with the IV → III transition observed between 36 and 41 °C. [e] Experiments for NO_3^- are performed in order of decreasing ν_r, i.e., decreasing t_c, with the III → IV transition observed between 28 and 31 °C.

angle of 54.736° as determined from the iterative fitting. Inspection of the ^{14}N MAS NMR spectra in Figures 1 and 2 which were recorded in order of increasing spinning speed clearly shows an abrupt change in the appearance of the manifold of ssbs for the NH_4^+ ion by increasing ν_r from 6000 to 7000 Hz. This is also reflected in the quadrupole coupling parameters (C_Q and η_Q) determined from analysis of the spectra (Table 1). This abrupt change is undoubtedly related to the phase transition from phase IV to phase III in NH_4NO_3, known to occur at about 35 °C and induced by the increase in frictional heating at the higher spinning speeds. A similar observation has been made in the ^{15}N MAS NMR study of $^{15}NH_4{}^{15}NO_3$ using a 5 mm probe.[8] From the data in Table 1, we observe that the phase transition results in a dramatic decrease by approximately 50% for both C_Q and η_Q in going from the low-temperature (phase IV) to the high-temperature phase (phase III), whereas the change in δ_{iso} (+1.7 ppm) is less pronounced. However, within the error limits determined for the isotropic chemical shifts, we find that the difference in $\delta_{iso}(^{15}N)$ (= +1.9 ppm) reported earlier for the $^{15}NH_4^+$ ion for this phase transition is identical to our determinations for the change in $\delta_{iso}(^{14}N)$ in this study. Clearly, the ^{14}N quadrupole coupling parameters (C_Q and η_Q) for the NH_4^+ ion determined from ^{14}N MAS NMR constitute a highly sensitive set of NMR parameters compared to the isotropic chemical shift in characterizing the studied phase transition.

^{14}N MAS NMR of NO_3^-. To characterize the phase transition in NH_4NO_3 just above room temperature by the behavior of the NO_3^- ion when subjected to ^{14}N MAS NMR spectroscopy, a sample of ^{15}N-enriched $^{15}NH_4NO_3$ was used. This material was selected in order to suppress the intensity of the $^{14}NH_4^+$ manifold of ssbs and thereby to better appreciate an undisturbed appearance of the manifold of ssbs for the NO_3^- ion. We should note that it is possible to obtain ^{14}N MAS NMR spectra for the NO_3^- ion without overlap of the NH_4^+ resonances and of sufficient quality using ordinary nonenriched NH_4NO_3 and an appropriate spinning speed. However, for the sake of clarity and for a more clear illustration of the ^{14}N spectral change which takes place during the phase transition, the ^{15}N-enriched $^{15}NH_4NO_3$ sample has been employed in the present study.

^{14}N MAS NMR spectra of the NO_3^- ion, acquired using a spectral width of 1 MHz and for ν_r equal to 4000 and 7000 Hz, are presented in Figure 3 parts a and c, respectively. These

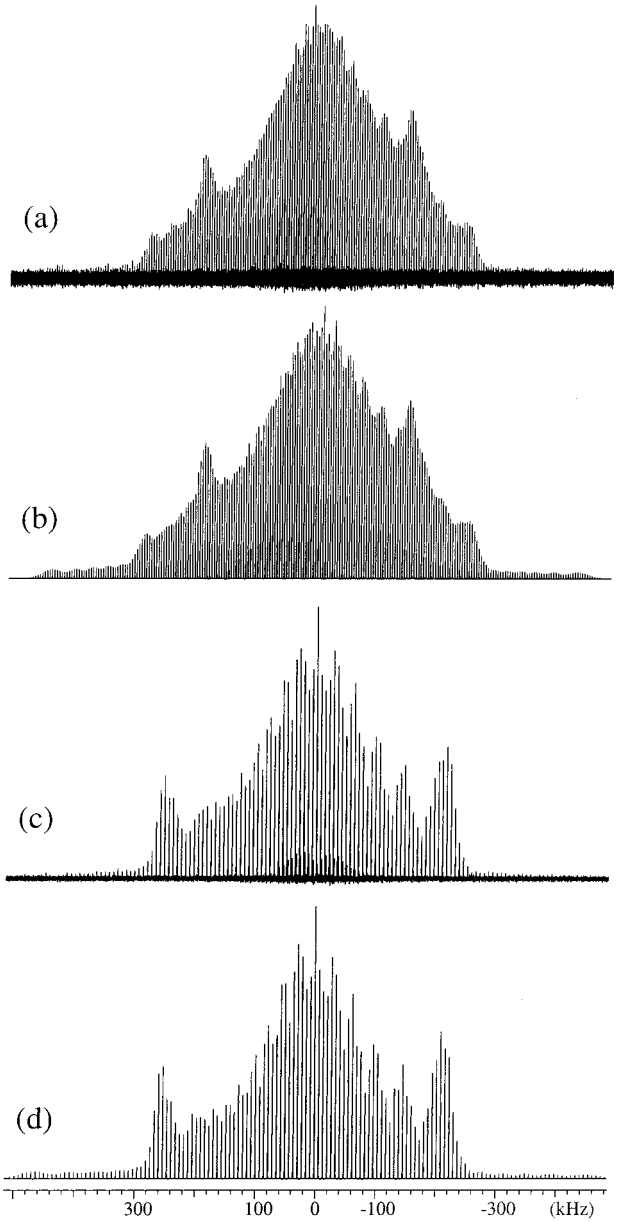

Figure 3. ^{14}N MAS NMR spectra of the NO_3^- ion in ^{15}N-enriched $^{15}NH_4NO_3$ illustrating the phase transition from phase IV to III in going from ν_r = 4000 Hz to 7000 Hz. (a) Experimental spectrum (phase IV) for ν_r = 4000 Hz, a line broadening of 10 Hz, and 40000 scans. (c) Experimental spectrum (phase III) for ν_r = 7000 Hz, a line broadening of 10 Hz, and 14659 scans. Parts b and d show the optimized simulated spectra corresponding to parts a and c, respectively, the parameters in Table 1, and for deviations from the exact magic angle of −0.012° parts a and b and −0.010° parts c and d. A low-intensity manifold of ssbs from the NH_4^+ ion (1% nonenriched) in phase III is observed in the experimental spectrum (part c; see text).

spectra exhibit clear differences in their overall appearances and can be used to characterize the ^{14}N quadrupole coupling parameters for the phase below (phase IV) and above (phase III) the phase transition at about 35 °C. The corresponding simulated spectra, based on the parameters resulting from the iterative fitting (Table 1) and using the ^{15}N CSA data reported elsewhere,[8] are shown in Figure 3 parts b and d below the experimental spectra. It is encouraging to observe that the spinning speed of 7000 Hz for the 7.5 mm probe induces a clear-cut and well-defined change in the ^{14}N spectral appearance and quadrupole coupling parameters for the NO_3^- ion as is also observed for the NH_4^+ ion (Figure 2c). Indeed the phase change

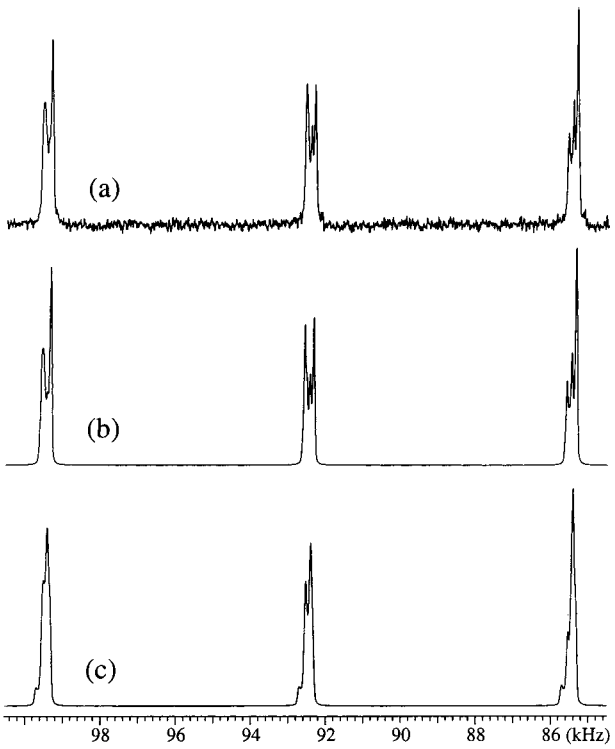

Figure 4. Expansions of spinning sidebands showing the line shape patterns for a selected region in the experimental (a) and simulated (b) spectra from Figure 3c,d. The simulated spectrum in b includes the second-order quadrupolar-CSA cross-term, whereas in the simulation c, this term has been omitted; otherwise identical parameters are employed (see Figure 3 and text).

for the NH_4^+ ion can also be observed in the centerpart of Figure 3c as the low-intensity manifold of ssbs resulting from the 1% $^{14}NH_4NO_3$ present in 99% ^{15}N-enriched $^{15}NH_4NO_3$.

To illustrate how the second-order quadrupolar-CSA cross term and the setting of the magic angle influence the ^{14}N spectra of the NO_3^- ion, Figures 4 and 5 show expansions and simulations for three of the ssbs observed in Figure 3c. Figure 4 shows that using the parameters in Table 1 the experimentally observed line shapes for these ssbs (Figure 4a) can only be simulated to high precision by inclusion of the quadrupolar-CSA cross term as seen in Figure 4b. When this cross-term is omitted, when all other terms in the average Hamiltonian are kept, and when the same parameters as for Figure 4b are used, the resulting simulation is shown in Figure 4c. The line shapes in Figure 4c clearly differ from those in Figure 4b and result from the second-order quadrupolar term modulated by the effect of the magic-angle setting. The influence of the adjustment of the magic angle on the same three ssbs is illustrated in Figure 5. The simulation in Figure 5b is identical to the optimized fitting (Figure 4b) for the experimental ssbs (Figure 4a) and corresponds to a deviation of $-0.010°$ from exact magic-angle setting. The simulations in Figure 5a−e, corresponding to deviations of -0.02, -0.01, $+0.00$, $+0.01$, and $+0.02°$ from the magic angle, illustrate that ^{14}N MAS spectra for the NO_3^- ion are sensitive to angle settings within a few thousands of a degree.

The clear-cut phase transition observed from the spectra for the NO_3^- ion leaves great promises to ^{14}N MAS NMR spectroscopy as a method in studies of phase transitions for nitrates in general. Finally, we should note that the difference in isotropic ^{14}N chemical shift determined in this study for the NO_3^- ion, $\Delta\delta_{iso}$ (^{14}N) = 3.5 ppm, in the transition from phase IV to phase III is similar to that reported by Anderson-Altmann and Grant[8] from the ^{15}N MAS NMR study, $\Delta\delta_{iso}$ (^{15}N) = 2.4 ppm, taking the error limits into account.

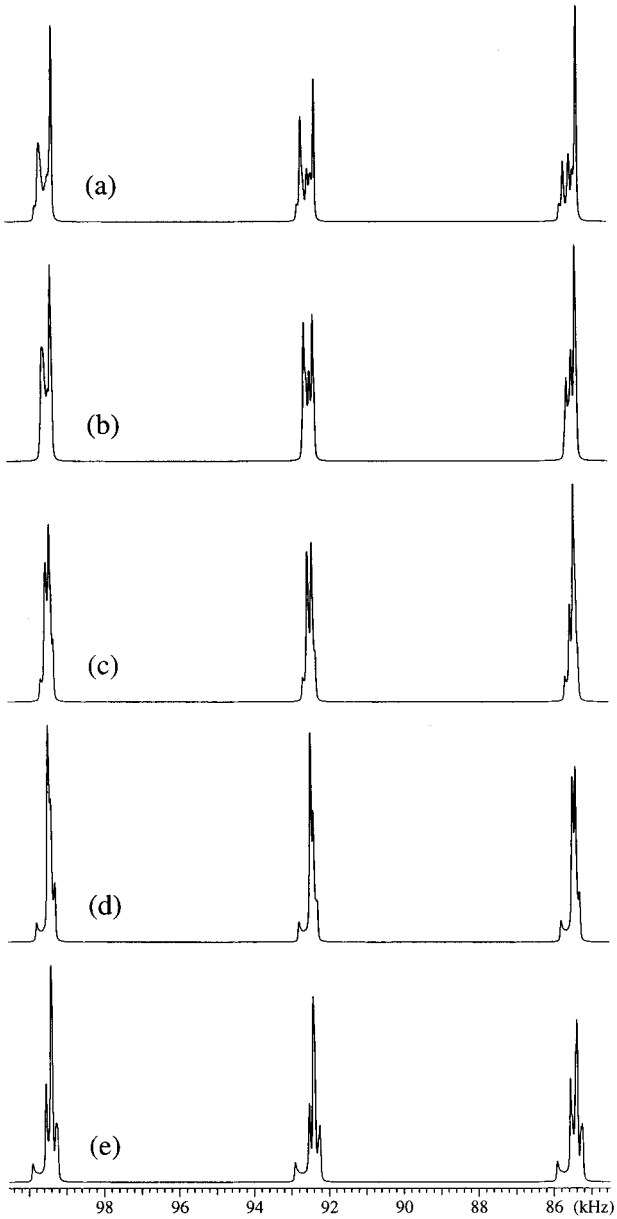

Figure 5. Expansions of simulated spinning sideband patterns illustrating the influence of magic-angle adjustment on the line shapes for the same three sidebands as in Figure 4. The simulations correspond to the following deviations from exact magic-angle setting: (a) $-0.02°$, (b) $-0.01°$, (c) $0.00°$, (d) $0.01°$, and (e) $0.02°$. The simulation in b is identical to Figure 4b, and all simulations employ the optimized parameters for the experimental spectrum in Figure 4a (Figure 3c).

Hysteresis. Following the determination of the phase transition for NH_4NO_3 from phase IV into phase III by means of ^{14}N MAS NMR at $\nu_r \approx 7000$ Hz, employing either the NH_4^+ or the NO_3^- ion (cf. Figures 2 and 3), we decided to investigate the possible effect of hysteresis (i.e., the thermal history of the sample) by ^{14}N MAS NMR using the NO_3^- ion as a probe. Thus, after acquisition of the spectrum for $\nu_r = 7000$ Hz (41 °C), ^{14}N MAS NMR spectra of the NO_3^- ion were acquired in decreasing order of ν_r for $\nu_r = 6000$ (36 °C, Figure 6a) and 5000 Hz (31 °C, Figure 6c), allowing 2−4 h to elapse before starting data acquisition overnight. These spectra appear quite identical to that obtained for $\nu_r = 7000$ Hz (41 °C), although minor intensity differences for the ssbs can be noted for the three spectra, caused by the change in spinning speeds. This

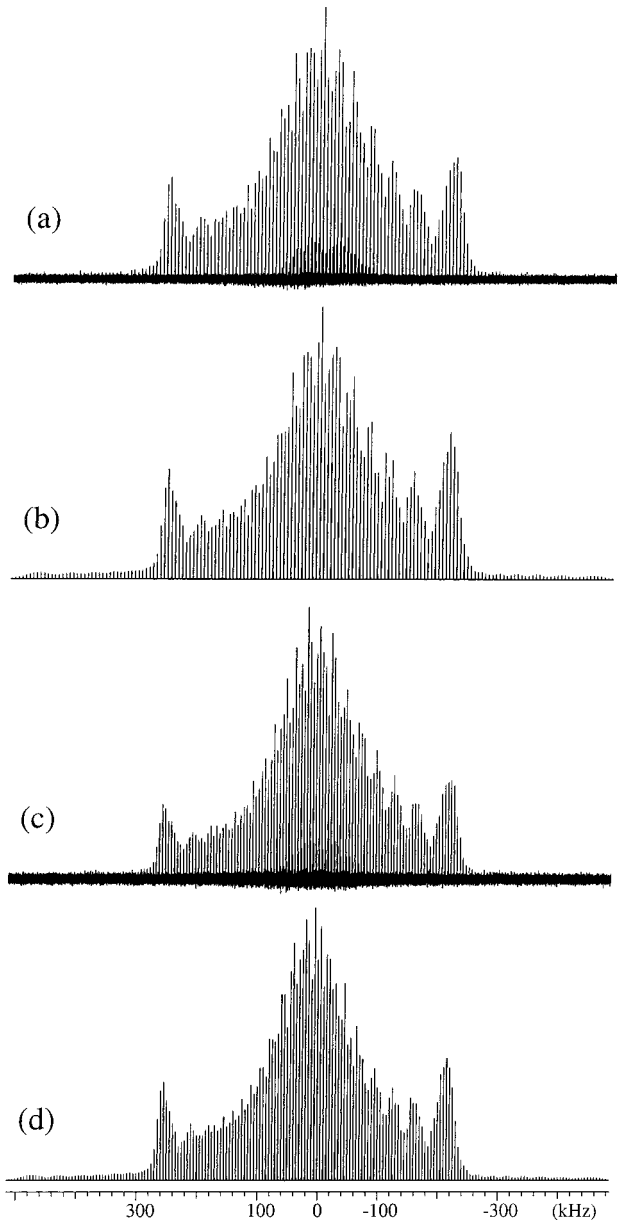

Figure 6. ^{14}N MAS NMR spectra of the NO_3^- ion in ^{15}N-enriched $^{15}NH_4NO_3$ for (a) $\nu_r = 6000$ and (c) 5000 Hz and recorded in order of decreasing spinning speed following the spectrum in Figure 3c for $\nu_r = 7000$ Hz and thereby illustrating the effect of hysteresis for the studied phase transition. (a) Experimental spectrum for $\nu_r = 6000$ Hz, a line broadening of 10 Hz, and 14336 scans. (c) Experimental spectrum for $\nu_r = 5000$ Hz, a line broadening of 10 Hz, and 16010 scans. Parts b and d show the optimized simulated spectra corresponding to parts a and c, respectively, the parameters in Table 1, and for deviations from the exact magic angle of −0.011° parts a and b and −0.010° parts c and d. See text.

shows that phase III still persists for $\nu_r = 5000$ Hz (31 °C) upon lowering the spinning speed. Furthermore, this same conclusion is reached by comparison of the shape for the low-intensity manifold of ssbs for the NH_4^+ ion in Figures 3 and 6 with the NH_4^+ ion spectra in Figure 2. However, decreasing ν_r to 4000 Hz (28 °C) and allowing the sample to stabilize its phase for about 4 h before starting acquisition of the ^{14}N MAS spectrum leads to a spectrum identical to that shown in Figure 3a. Thus, the phase transition for NH_4NO_3 just above room temperature exhibits the typical hysteresis behavior often encountered in phase transitions of solid inorganics (e.g., $AlPO_4$-cristobalite[17]) as well as organics (e.g., *d*-camphor[18]). An approximate temperature difference of about 8−10 °C for the phase transition temperature in the temperature range 30−40 °C depends on increasing or decreasing the sample temperature as seen from our results in Table 1.

^{14}N Quadrupole Coupling Parameters. Because of the quite large changes in both C_Q and η_Q for the NH_4^+ as well as the NO_3^- ion during the phase transition just above room temperature (about 34 °C) for NH_4NO_3 (Table 1), it seems of interest to compare these data with parameters determined for other ammonium salts and nitrates in the solid state. For this purpose, a comparison with parameters we recently determined from ^{14}N MAS NMR for a number of such compounds seems feasible.[1,19,20]

For the NH_4^+ ion (including alkylammonium ions), we have so far observed huge variations in C_Q ranging from 0 (NH_4Cl) to 1.2 MHz (ethylenediamine dihydrochloride). Furthermore, the variations for the asymmetry parameter are just as large ranging from $\eta = 0$ to 1. For example, for $NH_4H_2PO_4$, we find $\eta_Q = 0$, whereas for $(NH_4)_2HPO_4$, we obtain $\eta_Q = 0.9$ for the two nonequivalent NH_4^+ ions. Therefore, at this time, it appears difficult to come up with any structural relationships for the quadrupole coupling parameters of ammonium ions. On the other hand, however, the large variations observed for these parameters should make C_Q and η_Q extremely sensitive probes for characterizing phase transitions in ammonium salts. For the IV→III phase transition in NH_4NO_3, the 50% reduction, observed in this study for C_Q of the NH_4^+ ion, is ascribed to an increase in molecular reorientation for this ion in phase III. Finally, we should note that a ^{14}N MAS NMR spectrum of the NH_4^+ in NH_4NO_3 for $\nu_r = 7.8$ kHz, or at least part of it, has recently been published by Fung et al.[21] However, it appears impossible to achieve a simulated spectrum with an appearance resembling the published spectrum using either set of our parameters for the NH_4^+ ion (Table 1).

Comparison of the NO_3^- data (C_Q and η_Q) obtained for the two phases in NH_4NO_3 with those determined earlier for NO_3^- ions from ^{14}N MAS NMR[1] or reported in the literature[22] for KNO_3, $NaNO_3$, $Ba(NO_3)_2$, $Sr(NO_3)_2$, and $Pb(NO_3)_2$ appears somewhat more straightforward. For these nitrates, C_Q ranges from about 500 to 750 kHz, whereas $\eta_Q = 0$. For the two phases studied here for NH_4NO_3, the C_Q values fall in the centerpart of this range but differ mutually by only about 40 kHz. More interestingly, the clear visual difference in the appearance of the ^{14}N MAS NMR spectrum for the NO_3^- ion in the two phases (cf. Figure 3) shows that the change in η_Q from 0 to 0.25 is unique for the phase IV in NH_4NO_3 as compared to the other nitrates. Clearly, the asymmetry parameter η_Q by itself can be a very sensitive probe for characterizing or detecting phase transitions for quadrupolar nuclei in general. The slight increase observed for C_Q upon transition from phase IV to III indicates that the reorientational process (in-plane C_3 rotations) for the NO_3^- ion in the two phases is quite similar. From solid-state ^{15}N NMR studies of $^{15}NH_4{}^{15}NO_3$, it has been shown that this dynamic process first undergoes a dramatic rate increase upon transition from phase II to I.[6,8] Thus, the changes observed for the quadrupole coupling parameters (C_Q and η_Q) between phases IV and III is most likely related to differences in crystal structures for the NO_3^- ion in the two phases.

To gain further insight into a possible quantitative interpretation of the ^{14}N quadrupole coupling parameters for the NO_3^- ion in phase IV and III, the ^{14}N electric field gradients (EFGs) have been calculated for the NO_3^- ion in these phases employing point−monopole calculations. This approach has earlier proven useful in estimating the EFGs in ionic structures such as sodium

and cesium salts.[23,24] For the two phases of NH_4NO_3, only the geometry of the NO_3^- ion is taken into account in the calculations, employing the crystal structural data reported from neutron diffraction for the two forms of NH_4NO_3.[3,5] Assuming ideal charges for the oxygens of the NO_3^- ion (i.e., $q(O) = -2e$) gives the following ratio for the unique tensor element of the EFG tensor $V_{zz}^{calc}(III)/V_{zz}^{calc}(IV) = 1.03$ and EFG asymmetry parameters of $\eta_Q^{calc} = 0.02$ and 0.16 for phases III and IV, respectively. Alternatively, the effective charges of the oxygen atoms can be estimated from the crystal structures using the approach by Brown and Shannon[25] and the chemical bond data of Brown and Altermatt.[26] For phase III, this gives effective charges of $q(O1) = -0.507e$ and $q(O2) = -0.528e$, whereas $q(O1) = -0.653e$ and $q(O2) = -0.330e$ are calculated for phase IV of NH_4NO_3. Employing these charges in the point-monopole calculations gives the ratio $V_{zz}^{calc}(III)/V_{zz}^{calc}(IV) = 1.18$ and EFG asymmetry parameters of $\eta_Q^{calc} = 0.02$ and 0.58 for phases III and IV, respectively. The two calculated ratios for the unique tensor elements are in favorable agreement with the experimental ratio for the quadrupole coupling constants $C_Q(III)/C_Q(IV) = 1.07$. Furthermore, both calculations predict $\eta_Q \approx 0$ for phase III and a somewhat larger value of η_Q for phase IV as observed experimentally. These findings strongly suggest that the quite small variations in C_Q and η_Q for the NO_3^- ion upon the IV $\leftrightarrow$ III phase transition are related to the local geometries of the NO_3^- ion.

Conclusions

Solid-state ^{14}N MAS NMR spectroscopy is shown to be an excellent method in studies of phase transitions for nitrogen compounds. ^{14}N quadrupole coupling constants and asymmetry parameters for the NH_4^+ and NO_3^- ion in NH_4NO_3, as determined from the ^{14}N MAS manifold of spinning sidebands, are extremely sensitive to changes in crystal structure and dynamics induced by a phase transition. The quadrupole coupling data provide an alternative and more sensitive parameter set for characterizing phase transitions compared to the ^{14}N isotropic chemical shifts. For NH_4NO_3 the ^{14}N isotropic chemical shifts are identical to the corresponding ^{15}N values used earlier to characterize the solid phases from ^{15}N-enriched samples.

Acknowledgment. The use of the facilities at the Instrument Centre for Solid-State NMR Spectroscopy, University of Aarhus, sponsored by the Danish Natural Research Council, the Danish Technical Science Research Council, Teknologistyrelsen, Carlsbergfondet, and Direktør Ib Henriksens Fond, is acknowledged. Financial support from the two Danish Research Councils (J.nr. 5020-00-0018 and J.nr. 0001237) is acknowledged.

References and Notes

(1) Jakobsen, H. J.; Bildsøe, H.; Skibsted, J.; Giavani, T. *J. Am. Chem. Soc*. **2001**, *123*, 5098.
(2) Parsonage, N. G.; Staveley, L. A. K. *Disorder in Crystals*; Clarendon Press: Oxford 1978; p 338−350.
(3) Lucas, B. W.; Ahtee, M.; Hewat, A. W. *Acta Crystallogr*. **1979**, *B35*, 1038.
(4) Choi, C. S.; Prask, H. J.; Prince, E. *Appl. Crystallogr*. **1980**, *13*, 403.
(5) Choi, C. S.; Prask, H. J. *Acta Crystallogr.* **1982**, *B38*, 2324.
(6) Wasylishen, R. E. *Spectrochim. Acta* **1984**, *40A*, 115.
(7) Marino, R. A.; Bulusu, S. *J. Energ. Mater.* **1985**, *3*, 57.
(8) Anderson-Altmann, K. L.; Grant, D. M. *J. Phys. Chem.* **1993**, *97*, 11096.
(9) Schönwandt, B. V.; Jakobsen. H. J. *J. Solid State Chem.* **1999**, *145*, 10.
(10) Bjorholm, T.; Jakobsen, H. J. *J. Magn. Reson.* **1989**, *84*, 204.
(11) Jakobsen, H. J.; Skibsted, J.; Bildsøe, H.; Nielsen, N. C. *J. Magn. Reson.* **1989**, *85*, 173.
(12) Skibsted, J.; Nielsen, N. C.; Bildsøe, H.; Jakobsen, H. J. *J. Magn. Reson.* **1991**, *95*, 88.
(13) Skibsted, J.; Nielsen, N. C.; Bildsøe, H.; Jakobsen, H. J. *Chem. Phys. Lett.* **1992**, *188*, 405.
(14) Skibsted, J.; Nielsen, N. C.; Bildsøe, H.; Jakobsen, H. J. *J. Am. Chem. Soc.* **1993**, *115*, 7351.
(15) STARS is available as part of the VNMR software from Varian Inc.
(16) Spiess, H. W. In *NMR Basic Principles and Progress*; Diehl, P., Fluck, E., Kosfeld, E., Eds.; Springer: Berlin, 1978; Vol. 15.
(17) Philips, B. L.; Thompson, J. G.; Xiao, Y.; Kirkpatrick, R. J. *Phys. Chem. Minerals.* **1993**, *20*, 341.
(18) Yager, W. A.; Morgan, S. O. *J. Am. Chem. Soc.* **1935**, *57*, 2071.
(19) Jescheke, G.; Jansen, M. *Angew. Chem., Int. Ed*. **1998**, *37*, 1282.
(20) Unpublished results from our laboratory.
(21) Khitrin, A. K.; Fung, B. M. *J. Chem. Phys.* **1999**, *111*, 8963.
(22) Bastow, T.; Stuart, S. N. *Z. Naturforsch.* **1990**, *45A*, 459.
(23) Koller, H.; Engelhardt, G.; Kentgens, A. P. M.; Sauer, J. *J. Phys. Chem.* **1994**, *98*, 1544.
(24) Skibsted, J.; Vosegaard, T.; Bildsøe, H.; Jakobsen, H. J. *J. Phys. Chem.* **1996**, *100*, 14872.
(25) Brown, I. D.; Shannon, R. D. *Acta Crystallogr*. **1973**, *A29*, 266.
(26) Brown, I. D.; Altermatt, D. *Acta Crystallogr*. **1985**, *B41*, 244.